CONF-880887-14

UCRL-98175
PREPRINT

A Hard X-Ray Spectrometer for High Angular Resolution Observations of Cosmic Sources

C. J. Hailey
K. P. Ziock
F. Harrison
S. M. Kahn
D. Liedahl
P. M. Lubin
M. Seiffert

This paper was prepared for submittal to 32nd Annual International Technical Symposium on Optical & Optoelectronic Applied Science & Engineering San Diego, CA August 14-19, 1988

August 12, 1988

Lawrence Livermore National Laboratory

UCRL--98175

DE88 017005

A hard x-ray spectrometer for high angular resolution observations of cosmic sources

C. J. Hailey, K. P. Ziock

Lawrence Livermore National Laboratory, Laboratory for Experimental Astrophysics
P.O. Box 808, L-296, Livermore, California 94551

F. Harrison, S. M. Kahn, D. Liedahl

University of California, Department of Physics, Berkeley, California 94720

P. M. Lubin, M. Seiffert

University of California, Department of Physics, Santa Barbara, California 93106

ABSTRACT

LAXRIS (large area x-ray imaging spectrometer) is an experimental, balloon-borne, hard x-ray telescope that consists of a coaligned array of x-ray imaging spectrometer modules capable of obtaining high angular resolution (1–3 arcminutes) with moderate energy resolution in the 20- to 300-keV region. Each spectrometer module consists of a CsI(Na) crystal coupled to a position-sensitive phototube with a crossed-wire, resisitive readout. Imaging is provided by a coded aperture mask with a 4-m focal length. The high angular resolution is coupled with rather large area ($\sim$800 cm^2) to provide good sensitivity. Results are presented on performance and overall design. Sensitivity estimates are derived from a Monte-Carlo code developed to model the LAXRIS response to background encountered at balloon altitudes. We discuss a variety of observations made feasible by high angular resolution. For instance, spatially resolving the nonthermal x-ray emission from clusters of galaxies is suggested as an ideal program for LAXRIS.

1. INTRODUCTION

Since its inception, experimental astrophysics in the hard x-ray region (40–400 keV) has emphasized observations of high spectroscopic resolution at the expense of high angular resolution. To a large extent, this state of affairs can be traced to the lack of any real imaging capability at hard x-ray energies. Because reflective optics cannot be utilized above 10 keV and because true imaging electronic detectors have been largely unavailable in this range, most experiments have resorted to simple collimation, which limits resolution to $\sim$0.5 to 1°. With such low angular resolution, it is impossible to study in detail the angular distribution of hard x-ray emission from sources. The first step in developing an imaging capability in the hard x-ray region has recently been taken with the construction of a balloon-borne telescope with an angular resolution of 22 arcminutes (arc′).[1] This modest imaging capability allows measurement of the spectrum of the supernova SN1987A from 20 to 300 keV, free of contamination from LMC X-1, which is 36 arc′ away from the supernova.[2]

The instrument we are currently building, LAXRIS, will have an angular resolution in the 40- to 300-keV range of 1 to 3 arc′, considerably better than that achievable with any balloon- or satellite-borne experiments planned for the near term. Our high angular resolution is coupled with a rather large effective area; these characteristics make it feasible, for the first time, to perform a number of exciting and diverse observations. The following sections describe the overall instrument and payload design, sensitivity calculations, and science we anticipate doing.

2. OVERVIEW OF LAXRIS

LAXRIS consists of a high-Z-coded aperture mask and a position-sensitive detector plane consisting of approximately 50 scintillating crystals backed by imaging photomultiplier tubes (IPTs). The focal length of the telescope will be 4 m. Background rejection will be accomplished through the use of graded-Z shields and plastic scintillators. The entire telescope—consisting of masks, shielding, collimators, and detectors—will be mounted on a balloon-borne stabilized platform. We are currently designing and constructing the various LAXRIS elements.

At higher energies, coded aperture systems have previously operated in an Anger camera arrangement, in which separate crystal-phototube combinations function as individual spatial elements of the array.[3] Our modification of this design through the use of imaging phototubes has a couple of advantages:

- It leads to substantially higher angular resolution within a compact geometry.
- It provides significant redundancy because each detector can provide its own independent map.

The latter is particularly important for eliminating spurious systematic effects that can complicate the image inversion.

2.1. Detectors

The x-ray detectors consist of an alkali-halide scintillator crystal optically coupled to a commercial (Hammamatsu Photonics K.K.) IPT. An x-ray incident on the crystal is partially converted to scintillation light, which is converted to electrons on the IPT photocathode, which are amplified and collected on the resistively coupled, cross-wire anode. The ratio of charge signals collected on each of four preamplifiers can be processed to yield the centroid of the original light cloud, and hence the x-ray event position. The total summed signal from the preamplifers is proportional to the incident x-ray energy. We present some basic data on the detectors; more detailed discussions of their performance can be found in Ref. 4.

2.1.1. Energy and pulse-height resolution. The energy resolution and pulse-height linearity have been measured from approximately 14 to 122 keV. The energy resolution scales as $E^{-1/2}$, and the pulse-height linearity is excellent. The energy resolution at 100 keV is 10 to 11 keV for NaI(Tl) and 13 keV for CsI(Na).

2.1.2. Position resolution and linearity. The detectors show excellent position linearity over the active area of the IPT (~17 cm²). The position resolution is a function of crystal thickness, crystal type, and x-ray energy. Below the energy regime where Compton scattering is important, the resolution scales as $E^{-1/2}$. The dependence on crystal thickness is nonlinear because of the index of refraction mismatch between the crystal and the IPT entrance window. For NaI(Tl) and CsI(Na) crystals of thicknesses varying from 2 to 5 mm, the spatial resolution varies from 1 to 2 mm (FWHM) at 122 keV. NaI provides slightly better spatial resolution, but CsI has higher efficiency so crystal selection is coupled to the bandwidth and angular resolution desired in a particular observing program.

2.2. Coded aperture

The coded aperture is a shadow mask of opaque material with multiple pseudo-randomly selected apertures, which is placed in the x-ray path in front of the collimated imaging detectors. Post-processing of the detected counts in this configuration yields an image of the x-ray source distribution. In many situations, the angular resolution of such a system is close to that of a pinhole camera. However, multiple apertures can provide an open area of up to 50 percent of the total mask area, resulting in significant improvements in sensitivity over pinhole cameras. The application of coded aperture techniques to x-ray astronomy has been discussed extensively in the literature in the past few years.[5-7].

The coded aperture will be constructed out of tantalum. A thick mask is required for x-ray opaqueness, while small holes (~a few mm) are required for high angular resolution. This poses a construction problem because it is difficult to precisely cut square holes (round holes result in loss of area) of high aspect ratio in tantulum. We are investigating a novel fabrication technique in which the mask pattern is sandblasted into a thin glass substrate. Square tantalum slugs are then inserted into the sandblasted detents. This scheme will permit an open area of almost 50 percent.

2.3. Shielding—collimator

Background suppression will be accomplished by means of a passive, graded-Z shield and a plastic scintillator. The passive shield consists of 1 mm each of copper and tin and 2 and 3 mm of lead on the sides and bottom of the payload, respectively. These thicknesses were determined through a Monte-Carlo optimization of the instrument sensitivity for the background expected at balloon altitudes (see below). The plastic scintillator suppresses charged-particle background.

We are investigating several schemes for collimation but tentatively plan to use a collimator of tantalum sheet, approximately 20 cm high and overcoated with a layer of silver and copper, which will provide two-dimensional collimation of each detector pixel. This collimator will slightly reduce the effective area, but we have accounted for this in our simulations.

2.4. Telescope platform

We will base the telescope, consisting of masks, shielding, collimators, and detectors on a balloon-borne stabilized platform (Fig. 1). Because of the high angular resolution of the telescope, we will need a very accurate pointing system. A stabilized platform built for use with a millimeter-wavelength telescope is currently being adapted for LAXRIS. This platform has achieved 1- to 2-arc′ tracking in the lab. The goal is to improve the pointing stability to 30 arc″. A worse pointing stability can be tolerated if the pointing direction is known to this accuracy. An intensified CCD camera is currently being evaluated, which, in conjunction with a small optical telescope, can provide the requisite aspect information.

The pointing system uses three sensors for attitude determination; magnetometers for coarse absolute pointing to ~1°; an inertial guidance system consisting of gyros, accelerometers, and a navigation processor; and a CCD star camera for star tracking and gyro update. An onboard computer coordinates the gondola control. A torque-control reaction wheel controls azimuthal pointing, and a linear-force motor controls elevation. Ground control is handled by a full-duplex, dedicated telemetry system, which is separate from the balloon facility telemetry. An overview of the balloon electronics is shown in Fig. 2.

3. SENSITIVITY CALCULATIONS

A Monte-Carlo code has been written to model the response of LAXRIS to background and source fluxes. Various parameters can be selected, such as crystal, shield, and mask thickness, source strength and spectrum; integration time; detector area; energy resolution; and overall telescope geometry. Source x rays, cosmic-diffuse x rays, and atmospherically generated x and gamma rays are propagated through the shields, mask, collimator, and detector. Scattering, absorption, and fluorescent-emission processes in these telescope elements are followed to all orders. The anisotropy of the atmospherically generated photon background is fully taken into account in the model calculations. Aperture photons are assumed to pass through 3 g/cm² of residual atmosphere and a plastic anticoincidence shield on the coded aperture.

The predominant contribution to background is by extremely high-energy (400- to 1000-keV) photons, which leak through the shield and Compton scatter in the detector volume. Charged particles not vetoed by the plastic shields, neutrons, and natural radioactivity are not important compared to the Compton-scattered hard photons.

The program handles source photons in a like manner, determining detection efficiency for a given input-source spectrum. Figure 3 shows the five-sigma detection threshold for a continuum source accounting for all the relevant processes. For this calculation, we assume a 3-mm CsI(Na) crystal, 0.5° field of view, 10^4-s observation, 800 cm² of geometric area, and 20-keV bins.

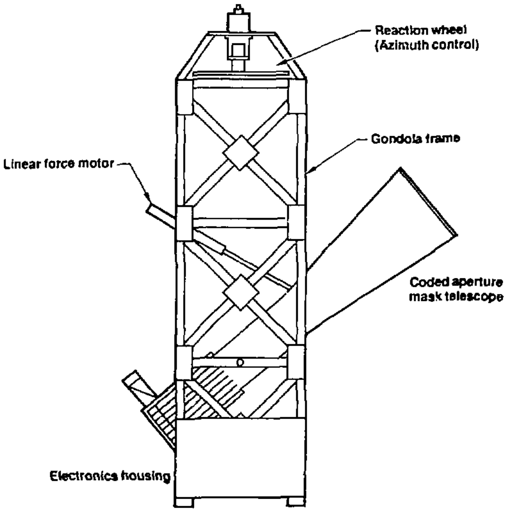

Figure 1. Overview of the LAXRIS telescope.

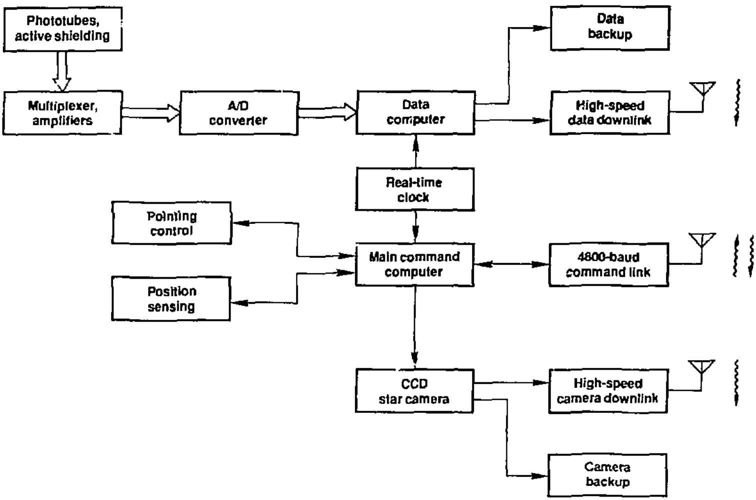

Figure 2. LAXRIS electronics block diagram.

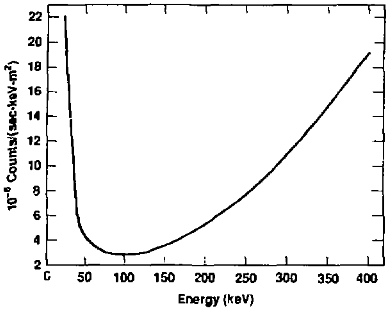

Figure 3. Five-sigma detection threshold for a continuum source observed with LAXRIS. Observing time is 10^4 s, and geometric area is 800 cm^2.

This Monte-Carlo was coupled to a program that treats reconstruction of coded aperture images of sources of a given energy spectrum and x-ray spatial distribution. It takes into account the relevant mask and detector operating parameters. Together, these two codes were used to predict the performance of LAXRIS.

4. SCIENTIFIC PROGRAMS WITH LAXRIS

Figure 4 shows the five-sigma detection threshhold for continuum emission as a function of power-law spectral index for the baseline LAXRIS design. The ordinate of the graph is the 50-keV energy flux, and the total bandwidth is 20 to 200 keV. The typical continuum sensitivity is seen to be about 1 milliCrab in the LAXRIS energy band. LAXRIS is substantially more sensitive than the HEAO-A4 experiment in the region of energy overlap. Potential targets for LAXRIS are discussed below.

4.1. Clusters of galaxies

At lower energies, the x-ray emission from clusters of galaxies is dominated by thermal radiation associated with hot gas gravitationally bound in the overall cluster potential. However, the spectra of the brightest clusters also exhibit a distinct nonthermal tail, which extends up to several hundred keV.[7-10] The nature of this nonthermal radiation is not well understood. It might be produced by very high energy electrons upscattering cosmic microwave background or optical photons into the hard x-ray band. Alternatively, it could be produced in the active nucleus associated with one or more of the individual member galaxies. Spatially resolving the hard x-ray emission can resolve this issue because the two models predict different intensity profiles. Even if extended emission is not detected, important constraints can be placed on such cluster components as the magnetic field and charged particles.[11]

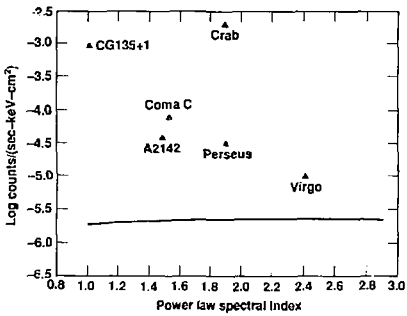

Figure 4. Five-sigma detection threshold (20- to 200-keV bandwidth) as a function of source spectral index (solid line). Results are referenced to continuum flux at 50 keV. Continuum fluxes for some potential targets are shown for comparison. Observing time and area are the same as in Fig. 3.

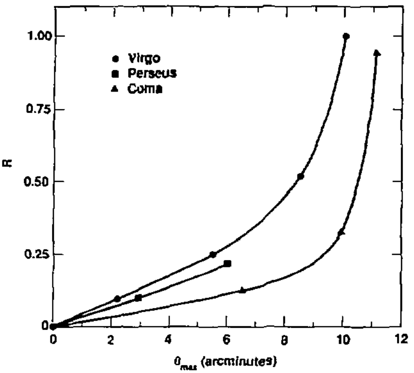

Figure 5. For x-ray emission of spatial extent $\theta_{max} \times \theta_{max}$ arc', the fraction (R) of total cluster x-ray emission that must be in the diffuse component for all image pixels to have four sigma detections. The diffuse emission is assumed to be uniform. Observation times: 10^4 s for Perseus and Coma, 8×10^4 s for Virgo. Pixel size is 2 arc'.

If the theories invoking inverse Compton scattering are correct, x-ray emission can be expected over scales comparable to radio emission. For Virgo, Coma, and Perseus (Fig. 5) this radio emission varies in extent from 6 to 28 arc'—amenable to observation with LAXRIS. The ability to image x-ray sources with a coded aperture is an extremely sensitive function of the spatial extent of the emission and the ratio of diffuse to total x-ray flux in the source. Figure 5 illustrates the maximum extent over which diffuse x-ray emission can be detected for three clusters, given various ratios (R) of diffuse x-ray flux to total x-ray flux. In each case, the emission is assumed to be uniformly spread over a region of the source θ_{max} by θ_{max} arc' in extent, and the R indicated is for a four-sigma detection in each 2-arc' pixel. For Perseus and Coma, a 10^4-s observation is assumed; and for Virgo, an 8×10^4-s (long-duration balloon) observation. The rapid decrease in sensitivity, if the x-ray emission is too extended, is apparent.

Figure 5 also shows Abell 2142, which is an interesting target because hard x-ray emission has been detected[6], but there is no obvious candidate object; several Seyfert galaxies lie within 20 arc' of the cluster center.

4.2. Galactic center and bulge

The galactic center is unobservable in the soft x-ray band, where imaging has previously been available, because of photoelectric absorption by dust in the galactic plane; the line of sight becomes transparent above 10 keV. Recently, two experiments have provided the first x-ray maps of this region at intermediate energies (5 to 25 keV).[12,13] In both were found a rather complex emission pattern, a number of discrete sources, and extended emission around the galactic center itself. Our experiment would provide a necessary complement to this work, because harder x-ray observations are required to select out the most energetic phenomena. The spatial and spectral distributions of the diffuse emission are of particular interest.

As has been pointed out by Grindlay et al.,[14] an imaging capability may be crucial in characterizing the hard x-ray spectrum of galactic-bulge x-ray sources because of the potential for non-imaging detectors to become source-confused in the central galactic bulge.

4.3. X- and gamma-ray source locations

With its high angular resolution, LAXRIS is capable of determining source locations with great accuracy. As an example, we mention the COS-B source CG 135 + 1. This object has been observed with a number of low-resolution hard x- and gamma-ray detectors.[15] Two candidates for counterparts have been identified, including a QSO and the radio source GT 0236 + 61. But the low angular resolution of the observations (~a few degrees) does not allow an unambiguous identification of one of these objects with the COS-B source. Each candidate requires invoking different models for the gamma-ray emission, either synchrotron self-Comptonization (QSO) or inverse Comptonization of stellar photons (GT 0236 + 61). LAXRIS can easily determine the position of CG 135 + 1 to a few arcseconds in less than 1000 s, completely resolving this ambiguity.

5. ACKNOWLEDGMENTS

This work was initiated with a grant from the Institute for Geophysics and Planetary Physics at Lawrence Livermore National Laboratory and from the University of California Office of the President (CALCOR) fund. We gratefully acknowledge their support.

This work was performed under the auspices of the U. S. Department of Energy by Lawrence Livermore National Laboratory under contract no. W-7405-Eng-48.

6. REFERENCES

1. M. R. Garcia, J. E. Grindlay, R. I. Burg, S. S. Murray, and J. W. Flanagan, IEEE Trans. Nucl. Sci. **33**, 735 (1986).
2. C. E. Covault, J. Braga, and J. E. Grindlay, Center for Astrophysics, Cambridge, MA, preprint no. 2659 (1988).
3. D. Palmer and T. A. Prince, IEEE Trans. Nucl. Sci. **NS-24**, 71 (1987).
4. C. J. Hailey, F. Harrison, J. H. Lupton, and K. P. Ziock, Lawrence Livermore National Laboratory, Livermore, CA, UCRL-98908 (1988), submitted to Nucl. Instr. Meth.
5. E. E. Fenimore and T. M. Cannon, Appl. Opt. **17**, 337 (1978).
6. E. E. Fenimore, Appl. Opt. **17**, 3562 (1978).
7. E. E. Fenimore, Appl. Opt. **19**, 2465 (1980).
8. S. Lea et al., Ap. J. **246**, 369 (1981).
9. A. Bazzano et al., Ap. J. **279**, 515 (1984).
10. F. Primini et al., Ap. J. **243**, L13 (1981).
11. C. D. Dermer and Y. Rephaeli, Ap. J. **329**, 687 (1988).
12. M. Kawai et al., Ap. J. **330**, 130 (1988).
13. G. Skinner et al., Nature **330**, 544 (1987).
14. J. E. Grindlay, M. R. Garcia, R. L. Burg, and S. S. Murray, IEEE Trans. Nucl. Sci. **33**, 750 (1986).
15. F. Perotti et al., Ap. J. **239**, L49 (1980).